Research Article

Qi Yao*, Mohammad Shabaz, Tarun Kumar Lohani, Mohammed Wasim Bhatt, Gurpreet Singh Panesar, and Raj Karan Singh

3D modelling and visualization for Vision-based Vibration Signal Processing and Measurement

https://doi.org/10.1515/jisys-2020-0123
Received Dec 09, 2020; accepted Jan 19, 2021

Abstract: With the technological evolutionary advent, a vision-based approach presents the remote measuring approach for the analysis of vibration. The structure vibration test and model parameter identification in the detection of the structure of the bridge evaluation occupies the important position. The bridge structure to operate safely and reliably is ensured, according to the geological data of qixiashan lead-zinc mine and engineering actual situation, with the aid of international mining software Surpac. To build the 3D visualization model of the application of visualization in mine production are discussed. The results show that the final solid model of -425 stope can accurately display the spatial form of each layer of stope through rotation, amplification and movement. The proposed system is effectually able to perform cutting, volume calculation and roaming in any direction, which has certain guiding significance for mine production management. An accuracy value of 98.75%, the sensitivity of 99%, specificity of 99.64% and PPV of 99.89% are achieved using the proposed 3D modelling and visualization algorithm for vibration signal processing and management.

Keywords: 3D modelling, vibration signal processing, vibration measurement, 3D visualization, reliability

1 Introduction

With the rapid development of the national economy, in order to promote further economic development, promote cultural exchanges, strengthen national unity, reduce regional differences, and consolidate national defense, the transportation industry has been vigorously developed, and modern transportation networks have been established in all parts of the country [1]. As an important part of road transportation, bridge engineering in China has been among the world's advanced in both construction scale and science and technology after decades of efforts. Overpasses and viaducts with various functions and beautiful shapes, as well as super-span Bridges spanning the Yangtze River, Yellow River and other large rivers, have sprung up and been built frequently. With the progress of science and technology and the improvement of economic, social and cultural level, people have put forward higher requirements for bridge construction. Bridges in the whole operation service period, not only inherit the earthquake, wind, water, corrosion and other natural environment, and caused by a lack of maintenance, maintenance is not timely, vehicle crash, a surge in traffic, vehicle overloading, the influence of such factors as bridge structure is easy to produce all kinds of damage, reduce the bearing capacity of the bridge and operation condition, and even affect the operating

***Corresponding Author: Qi Yao:** Changzhou College of Information Technology, Changzhou 213164, China; Email: qiyaochangzhou@gmail.com
Mohammad Shabaz, Raj Karan Singh: School of Computer Science Engineering, Lovely Professional University, India
Tarun Kumar Lohani: Arba Minch University, Ethiopia
Mohammed Wasim Bhatt: Department of Computer Science Engineering, Central University of Punjab, India
Gurpreet Singh Panesar: Department of Computer Science Engineering, Chandigarh University, India

safety, continuous bridge accidents occurred in recent years, caused many casualties and huge property losses, is a wake-up call to the people [2]. Therefore, in order to ensure the bridge structure can operate safely and reliably and avoid the occurrence of structural disaster, it is necessary to carry out comprehensive detection, evaluation and health monitoring of the bridge structure's use state. To evaluate the state of the bridge structure, it is generally to judge the health state of the structure by means of bridge appearance inspection, bridge non-destructive testing, static load test and dynamic load test. Bridge structure dynamic load test to determine the dynamic performance of the structure of the bridge, the performance is important symbol, the bearing capacity of bridge operation state, and it is the basic principle of structural damage will cause the system mass or stiffness change, resulting in the change of the model parameters, so it can be through the change of the model parameters to determine, evaluate structural damage [3].

Vibration signal processing and measurement also plays an important role in monitoring the rotational machineries in the industrial applications. It is desirable for monitoring the conditions, fulfilling the maintenance requirements, fault prognosis and diagnosis in several industrial processes. The decision support system for vibration signal processing and analysis is depicted in Figure 1, which involves three stages of acquiring, processing and analysis.

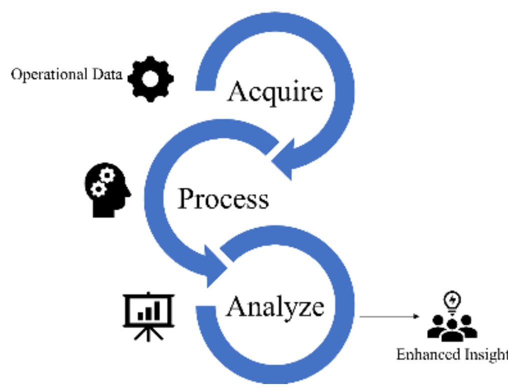

Figure 1: Decision support system for vibration signal processing

Over the last few decades, the usage of sensors and image processing modules has gained the interest of researchers for vibration measurement [4–6]. The rapid development of imaging sensors and 3D modeling and visualization algorithms encourages the vision-based alternatives for vibration measurement comparative to the conventional methods [7–9]. The object recognition and tracking systems have been used to achieve high measurement performance while maintain a tradeoff with the computational complexity [10, 11]. It is suggested in various recent works that for the evaluation of bridge structures, it is necessary to analyze the static load test as well as action load tests for dynamic structure estimation. Therefore, in order to carry out a comprehensive detection and evaluation of the bridge structure, this work utilizes not only static load test on the structure, but also in-action load test on the structure, identify the dynamic parameters of the structure, and verify the actual running state of the structure from multiple angles.

1.1 Contribution

This article proposed a polynomial fitting edge gray curve edge detection method for the measurement and analysis of high frequency vibrations. The ordinary object detection techniques possess the limitation due to the utilization of ordinary digital cameras which makes it difficult to meet the requirement of high frequency analysis of vibration. This shortcoming is effectively addressed in this work. The structure vibration test and model parameter identification in the detection of the structure of the bridge evaluation is discussed in this paper. The bridge structure to operate safely and reliably is ensured as per the geological data of qixiashan lead-zinc mine and by analyzing the engineering actual situation using international mining software Surpac. The application of visualization in mine production are discussed in order to build the 3D visualization model. The experimental results demonstrate the performance of high speed system for accurate detection of vibration signals. The outcomes obtained depicts that the final solid model of −425 stope can accurately display the spatial form of each layer of stope through rotation, amplification and movement. The proposed system is able to perform cutting, volume calculation and roaming operations in any direction which is certainly significant in mine production management systems.

1.2 Organization

The rest of the paper is organized as: Section represents the recent work carried out in the field of 3D modeling and visualization based vibration analysis systems. The construction of 3D model based on engineering methodology is discussed in Section 3. The stepwise 3D modeling and visualization of engineering geology based on Surpac Vision is presented in Section 4 which is followed by the conclusion in Section 5.

2 Literature review

Digital image processing technology uses computer to convert image information into digital information and process the digital information so as to obtain more information from the image information. At present, digital image processing technology has been applied in many fields, such as quality inspection of industrial production, satellite remote sensing and aerial measurement, medical diagnosis and so on. The principle of digital image processing technology for vibration test is: acquire image information by collecting video, obtain vibration track field of the measured object by image processing technology, and then conduct spectrum analysis of the vibration track field to obtain vibration parameters. Compared with the conventional vibration test, this method has no contact with the tested structure, high precision, good repeatability, convenience and speed, and low equipment input. Digital image processing technology based on road engineering structure is an accurate measurement of structure vibration. The dynamic displacement monitoring technology based on machine vision has developed rapidly in recent years due to its advantages of non-contact, real-time, remote and portability. Xu, F. proposed a multi-objective displacement monitoring method based on machine vision technology. The template matching algorithm and multi-target displacement calculation method based on digital image processing technology are introduced in detail. Using industrial digital camera and high power zoom lens, the \r\NA single point multi-target displacement monitoring system is developed by MATLAB. The results show that the single point multi-objective displacement monitoring method based on machine vision technology is feasible and suitable for synchronous multi-point vibration or rotational displacement monitoring of large structures [12]. Pit and groove is the most common form of damage of cement concrete pavement, which will affect the safety and drivability of pavement. Therefore, timely and accurate hole detection is an important task to make correct maintenance strategy and ensure driving safety. Gao, X. *et al.* proposed a method combining grayscale and texture feature processing. The method is mainly combined with industrial camera to realize fast and accurate detection of tunnel. Image processing techniques include texture filters, image grayscale, morphology, and maximum connected domain extraction in collaboration to extract useful features from digital images. A pit machine learning model based on support vector hangar (LIBSVM) is constructed to distinguish longitudinal crack, transverse crack and complex crack. The method was verified by using the data of Inner Mongolia agricultural and pastoral area. Through the comprehensive identification experiment, the recall rate is 100%, precision rate is 97.4%, f1 is 98.7%. In addition, the overlap rate between the extracted area and the original image is estimated. Images with an overlap rate of more than 90 percent accounted for 76.8 percent of the total images, and images with an overlap rate of more than 80 percent accounted for 94 percent of the total images. The comparison shows that this method is superior to the existing methods not only in the accuracy of pit detection, but also in the segmentation effect and processing efficiency [13]. Gao, X. *et al.* proposed a rf vortex beam deviation measurement method based on image processing. Theoretical analysis and numerical simulation of deviation OAM wavefront show that deviation information can be measured by extracting the characteristics of OAM mean value distribution and variance distribution. It is found that the extreme values of mean OAM distribution and variance distribution correspond to tilted singularities and original fulcrum respectively. These extreme points can be found by the image processing algorithm of recognizing circular spots. A proof-of-concept experiment is presented, in which a 2-D scanning probe is used to measure a 10-degree dip OAM beam under mode +1. The tilt measurement error is only 0.39 degrees [14].

Park *et al.* [15] proposed a vision-based approach for the measurement of displacement and the model presents satisfactory results. Ye *et al.* [16] presented three dimensional architectures for the measurement of displacement by making use of two-dimensional technique of digital image correlation. Becker *et al.* [17] proposed a DIC based monitoring system in order to measure the tensile force of cable. Their designed system attains better accuracy for measuring the strength cable of a cable stayed bridge. Ye *et al.* [18] proposed a camera-based approach for the measurement of dynamic displacement in large scale structures. A three-dimensional displacement measurement approach was proposed by Quan *et al.* while utilizing the two-dimensional digital image correlation (DIC) method [19]. Another vision-based vibration monitoring approach utilizing DIC was proposed by Kim *et al.* for the evaluation of cable tensile forces in the cable stayed bridges [20]. A camera-based sensor system providing robust object search, was proposed by Fukuda *et al.* [21] for the measurement of dynamic displacement of large-scale structures. To overcome the restriction of ordinary digital cameras (which fails to analyze the high frequency vibration), high speed camera systems have been utilized [22–24]. The model identification was realized for simple structures by Chen *et al.* [23] while utilizing phase based optical flow as well as motion magnification methods for the monitoring of high-speed videos. A damage detection method was proposed by Cha *et al.* [24] for phase-based motion extraction, while Kalman filter was utilized for the detection of damages in the structural system using the high-speed vision analysis. An efficient solution was provided by the utilization of phase based optical flow [23–27] beneficial for the estimation of velocity at different image sequence points. There are several template matching algorithms like normalized cross-correlation (NCC) [30], sum of squared differences, etc. which scans the predefined template of the entire image in roder to find the best match. Various researchers adopted enhanced correlation coefficient (ECC) algorithms [28] and up-sampled cross correlation (UCC) for image registration purposes. Image interpolation, fast Fourier transform and different up-sampling operations increases the computational burden making these methods not that much suitable for real-time measurement in the systems equipped high-speed sensors [29–31].

The limitation with the approach is the utility of ordinary digital cameras which makes it difficult to meet the requirement of high frequency analysis of vibration. In this paper, polynomial fitting edge gray curve edge detection method is proposed which can measure the high frequency vibration analysis. The experimental results demonstrate the performance of high speed system for accurate detection of vibration signals.

3 Construction of 3D model of engineering geological body

Nanjing Qixiashan lead-zinc mine is located in Qixia Town, Nanjing city. The mineral composition of the mine area is mainly galena, sphalerite, pyrite, siderite and calc-siderite. It is followed by tetrahedrite (including arsenotetrahedrite and silver-containing tetrahedrite), chalcopyrite, pyrite and a small amount of magnetite, siderite, ferrosiderite, arsenopyrite and pyrrhotite. Gangue minerals are mainly quartz and calcite (including manganese calcite and manganese calcite) [32, 33]. The second is dolomite, manganese dolomite, iron dolomite, chalcedony, and barite. The most common ore structures are granular structure, Mosaic structure, metasomatic structure, metasomatic residual structure and microcrushing structure. The ore structure is mainly brecciated, blocky and disseminated, followed by veined, reticulated and banded. Other structures such as lamellar structure, colloidal structure, crumpled structure, crystallographic structure, residual structure, comb structure and so on are relatively rare. The natural types of ores are mainly brecciated ores (about 35% of the total ore), block ores (about 30% of the total ore) and disseminated ores (about 25% of the total ore). Other types such as veins, reticular veins, clumps and bands are less abundant, accounting for about 10% of the total ore. The mine uses the upward horizontal slicing point column filling mining method, leaving not only the top and bottom column, but also the middle column and the point column. Under the circumstance of shortage of lead-zinc resources and still need to be imported, to further improve the utilization rate of ore resources, it is necessary to find technically feasible and economical mining methods and corresponding technology under the mining technology condition of deep ore deposits, and to carry out engineering technical transformation of deep ore body mining. The 3D geological model has some guiding significance for mining design, production schedule planning, production management, resource report analysis and intelligent optimization. Therefore, it is very necessary to establish accurate and realistic 3D geological entity model.

4 Results of 3D modeling and visualization of engineering geology based on Surpac Vision

Building 3D solid model (3DM) based on Surpac can be generally divided into the following processes: 1) Drawing line string, editing line string and line string layer cleaning; 2) Connecting line string, creating triangle network; Definition and editing of entity model attributes. The process is shown in Figure 2.

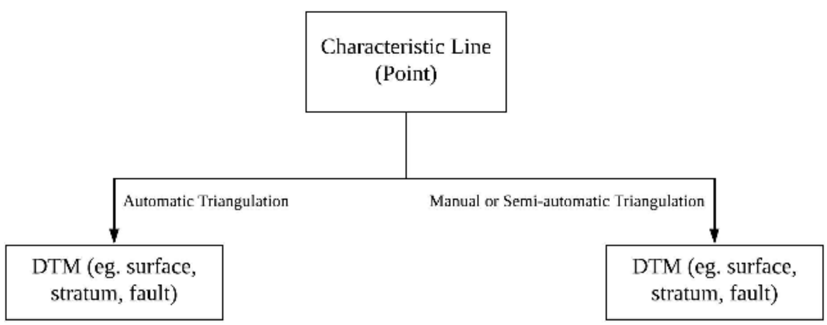

Figure 2: Flow chart of entity model construction

4.1 Construction of stope solid model

4.1.1 Construction of each layered entity model in stope

The construction of stope solid model is very important for mine production management. Combined with roadway model, the established stope solid model can clearly and intuitively display the three-dimensional spatial distribution among various layers of stope, the geological bodies in stope, such as ore passes, air traps, filling Wells and roadways. According to the actual situation of Qixiashan Lead-zinc mine in Nanjing, the 7th layer of stope 1015 interrupted by −425 is taken as an example. The actual CAD chart is used to construct the solid model of stope layer. The specific steps are as follows: 1) Treatment of stratified geological plan of stope. The seventh stratified geological plan of stope was screened by line segments, and only stope boundary and ore pass, filling well and civil air defense well were retained, and the stratified line file of stope was generated. 2) Reset the graphics workspace, delete the repeating points, repeating segments and clustering nodes in the layer, and clean up the layer layer of stope. 3) Edit the layering line file of stope, so that all line segments in the layer must be closed, without repeat points, intersections, clustered nodes, etc., and the peripheral line (stoping limit) is clockwise, while all lines inside (point column, civil air defense well, pass, and filling well boundary line) are counterclockwise; 4) The three-dimensional solid model of stope is constructed, as shown

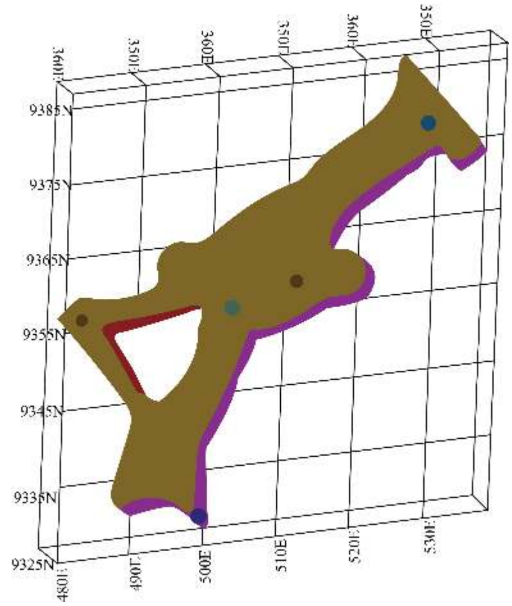

Figure 3: The seventh layered three-dimensional solid model of stope indicating Stope 1015

in Figure 3. In the figure, the brown hole represents the air defense well, the turquoise hole represents the pass well, the blue hole represents the filling well, and the red area is the point column [34, 35].

4.1.2 Construction of roadway solid model

By dividing the stope each layered entity model and physical model of roadway together, at the same time display in the window interface, can be more intuitive image the reaction of the stope each hierarchical spatial distribution form, at the same time can also be intuitive reaction between mining and roadway space position distribution of auxiliary mining design and production management [36]. This paper constructs a solid model of roadway based on roadway contour method. The steps of building roadway model are basically the same as

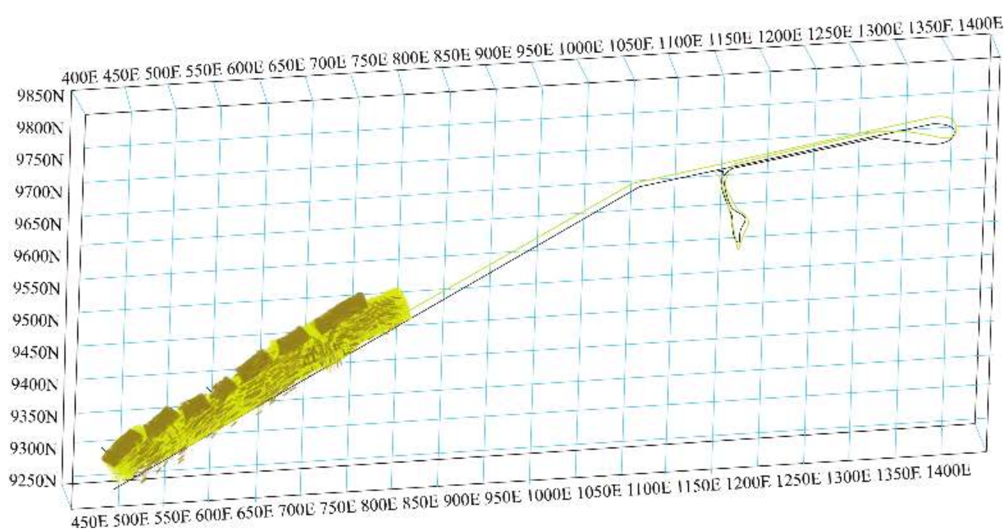

Figure 4: Solid model of stope and roadway in the middle section indicating stope −425

those of building stope layered model. The final constructed solid model of −425 middle tunnel is shown in Figure 4.

4.2 Construction of ore body grade model

The solid model constructed by software can visualize the spatial distribution of geological bodies (such as roadway, stope, etc.) and the three-dimensional coordinates of each point. For mining designers and production managers to understand the characteristics of the geological properties and its intrinsic change rule is very necessary to build the block model and the grade of ore body model not only has the advantage that the entity model, and can intuitively show the inherent characteristics of the geological body image attributes, and sums up the internal change law of geologic body, therefore, in the process of mining design and production management, on the basis of the entity model of the ore bodies, building block model of ore body and grade model is very necessary. Block model building is the basic idea of the geological body or ore bodies according to certain block of size is divided into many small cuboids and used to approximate representation of the geological body or ore bodies, each block of small cuboid has the corresponding properties of geological body or ore body internal properties of a certain position, all the rectangle unit block properties change rule are the internal change rule of the geological body or ore body [37]. The geological body or ore body piled with this cuboid unit block is called block model. In the block model, there is no requirement for the size of the cuboid unit block. The largest block in the block model is called the parent block, and the small block formed by the parent block is called the child block. When the block model of Qixiashan lead-zinc deposit in Nanjing is constructed, the solid model of the ore body is used to constrain the block model, which makes the block model more vivid.

4.2.1 Grade model construction

The grade model is mainly based on the following data: the solid model reflecting the spatial position of geological bodies, the sample combination file revealing the properties of geological bodies, etc. To sum up, the process of building grade model is shown in Figure 5.

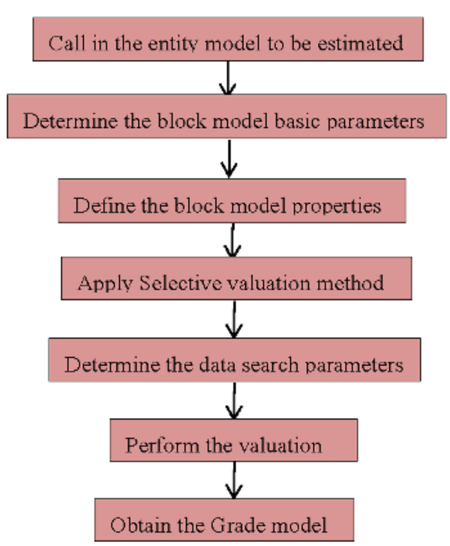

Figure 5: Flow chart of grade model construction

4.2.2 Define the parameters of the block model

The various steps involved in defining the parameters of the block model are described in the sequential steps as follows.

Step 1: Determine the scope of the sulfur ore solid model
Open the sulfur ore entity model and run the menu: query the range of the reporting layer to obtain the range of the sulfur ore entity model. Determine the range of the sulfur ore entity model as suggested in Table 1.

Table 1: Ranges of the sulfur ore entity model

Ymin=9270.368	Ymax=9569.311
Xmin=367.593	Xmax=878.933
Zmin=−681.699	Zmax=−103.345

Step 2: Define the scope of use of the block model
There are three ways to define the use range of block model: minimum/maximum coordinates, origin coordinate range, and range from line file. The “minimum/maximum coordinates” and “origin coordinates/range” are interoperable, and you can choose any of the three methods. Considering that the block model completely encloses the geological body entity model, the “minimum/maximum coordinate” method is adopted, and the block model is defined as expressed in Table 2.

Table 2: Ranges of scope for block model

Ymin=9200	Ymax=9600
Xmin=360	Xmax=900
Zmin=−700	Zmax=−100

Step 3: User block size
The size of the user block depends on the purpose of using the model, reference to the situation of the data space, such as level control, resource calculation, open-pit mine optimization, etc. The user block size is a determinant of the size of the interpolated block. In general, in the XY plane, the size of the block is generally 1/3 to 1/5 of the exploration line spacing, and in the Z direction, the size of the block is generally 2-3 times of the combined sample length or one part of the integral step height. But it must be an integer block within the block model. According to the shape of the sulfur ore body and the engineering control network, the user block size is defined as: 10×10×5.

Step 4: Sub-block and minimum size
The standard sub-module and variable sub-module are set in the software. In the standard sub-module, the secondary module is defined to be subdivided in a consistent proportion in three directions, but in the variable sub-model, different proportions can be used for subdivision in three directions respectively. The maximum

number of blocks that can be owned along each edge of the model must be a multiple. In this paper, standard secondary modules are selected, and the minimum block size is defined as: 5×5×2.

To run the program to get the results as shown in Table 3, the table shows that sulfur qixiashan ore block model of minimum coordinate, maximum coordinate, user block size, the minimum block size, location, Angle and pitching Angle, a unit of the total, keep information, such as the efficiency of the unit, a total of 1635 blocks of storage efficiency is as high as 99.92%, this shows that the cell block alignment is very high, and the real model defined by the block model parameters is very reasonable.

Table 3: Block model summary

Minimum coordinate value	Y=9200	X=360	Z=−700
Maximum coordinate value	Y=9600	X=900	Z=−100
User block size	Y=10	X=10	Z=5
Minimum block size	Y=5	X=5	Z=2.5
Rotating	Bearing: 0	Angle: 0	Pitching Angle: 0
Total No. (block)		1635	
Storage efficiency (%)		99.92	

4.2.3 Properties of block model

After building the block model, set the block model constraint information, as shown in the table. After loading the constraint, the sulfur ore block model can be obtained as shown in the Figure 6 and Figure 7. Based on the sulfur block model, the grade value of sulfur element is filled to build the grade model of Qixiashan sulfur mine in Nanjing. The basic idea is: fill the line file with borehole data generated by combined samples into the block model by using the inverse ratio method of distance, assign values to the block model, and get the sulfur ore grade model.

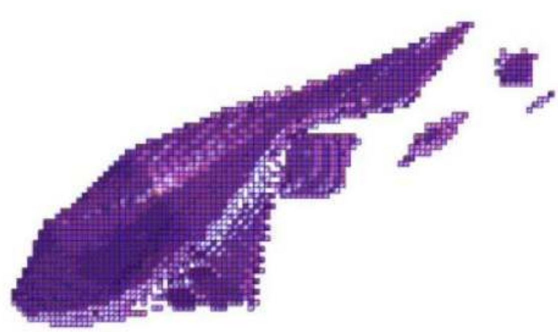

Figure 6: Model of sulfur ore block

In Surpac software, in order to show the sulfur grade distribution more clearly, different grades are displayed in different colors according to the properties of model coloring. The grade value of each unit block can be inquired arbitrarily in the grade model of sulfur ore, so that the distribution of sulfur grade in the ore body can be visualized.

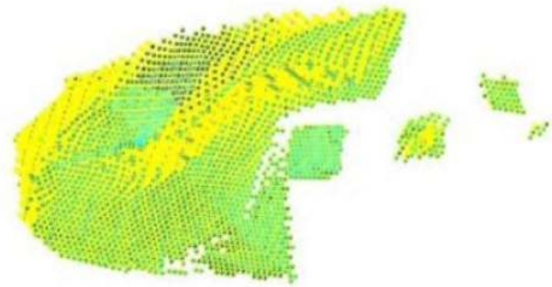

Figure 7: Grade model of sulfur ore after coloring by attribute

4.2.4 Evaluation in terms of various performance indices

The performance of the improved 3D modeling and visualization for vibration signal processing and measurement is evaluated in terms of various performance indices. These indices are obtained from the true and the predicted values of correct vibration measurement. Accuracy, sensitivity, specificity and positive prediction value (PPV) are evaluated for the proposed algorithm using the values of true positives (TP), true negatives (TN), false positives (FP) and false negatives (FN) and are given by equation 1 to equation 4.

$$\text{Accuracy} = \frac{TP + TN}{TP + FP + TN + FN} \tag{1}$$

$$\text{Sensitivity} = \frac{TP}{TP + FN} \tag{2}$$

$$\text{Specificity} = \frac{TN}{TN + FP} \tag{3}$$

$$\text{Positive Prediction Value} = \frac{TP}{TP + FP} \tag{4}$$

Figure 8 depicts the obtained values of the performance indices for the proposed 3D modeling and visualization algorithm for vibration signal processing.

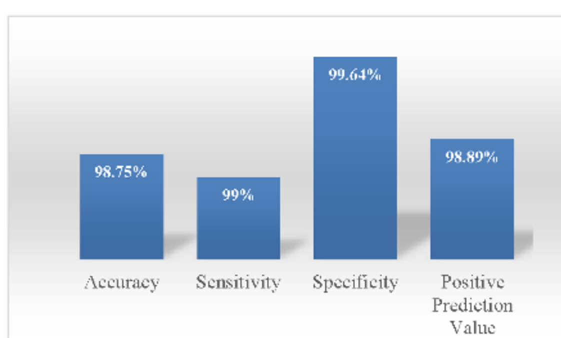

Figure 8: Performance Evaluation Indices

From Figure 8, it is seen that accuracy value of 98.75% while providing sensitivity of 99%, specificity of 99.64% and positive prediction rate of 98.89%. The sensitivity rate of 99% reveals the efficiency and capability of the proposed algorithm for identifying the vibration signals. The comparative analysis of the proposed 3D modelling and visualization for vibration signal processing and measurement with the latest state-of-the-art method is depicted in Figure 9.

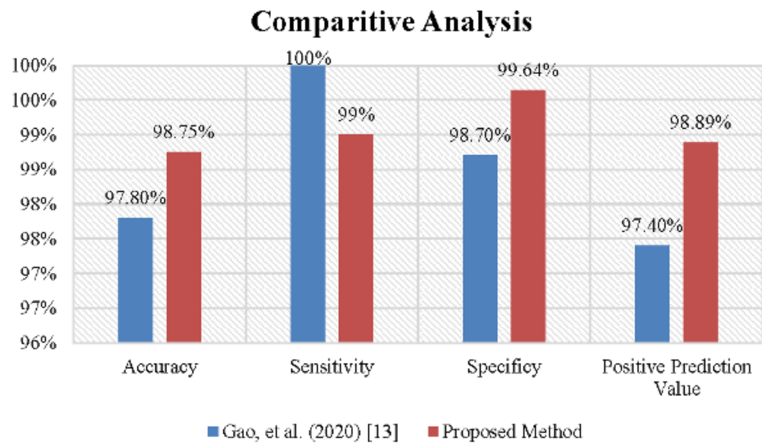

Figure 9: Comparative analysis of the proposed technique with latest state-of-the-art method

From Figure 7, it is revealed that the proposed 3D modelling and visualization for vibration signal processing and measurement approach outperforms the latest state-of-the-art method in vibration signal processing, thereby providing the maximum accuracy of 98.75% comparative to the existing method.

5 Conclusion

This paper analyzes and studies the principle and method of constructing the 3D visualization model of the geological body with the help of international mining software Surpac. This study utilizes the geological data and engineering practice of Qixiashan Lead-zinc mine in Nanjing. This paper preliminarily discusses the application of the 3D visualization model in mine production visualization. The main contribution and conclusions drawn from the study are as follows:

1. According to the geological information collection and mining engineering actual situation, stope three-dimensional entity model for the visual analysis. The article builds the layered solid model of the stope and the roadway model −425, eventually form −425 middle stopes solid model. Through the rotation, zoom, mobile, etc., can be precisely displayed stope each layered space form the cutting can be arbitrary direction, volume calculation, such as the mine production management is of certain guiding significance.
2. Based on the solid model of Qixiashan ore body in Nanjing, this paper analyzes the building principle of block model. This paper also studies the building method of block model, uses the inverse ratio method of distance to the block model and constructs the grade model of the ore body, and discusses the application of grade model in mines. An accuracy value of 98.75% is achieved for the proposed 3D modeling and visualization algorithm for vibration signal processing and management.

The proposed system is effectually able to perform the cutting operation, volume calculation as well as roaming in any direction, that has a guiding significance in mine production management. In future, the authors will strive for more reliable and feasible solution for vibration signal processing and management using the combination of image processing and 3D modelling.

References

[1] Cui, X., Li, C., Geng, Y., Ge, W., & Zhang, Z. (2019). Secondary envelope extraction based on multiple hilbert transforms for laser self-mixing micro-vibration measurement. Applied Optics, 58(34), 9392.

[2] Yang, G., Wu, J., & Hu, Q. (2019). Rapid detection of building cracks based on image processing technology with double square artificial marks. Advances in Structural Engineering, 22(5), 1186-1193.
[3] Jing, J., Huang, M., Li, P., & Ning, X. (2018). Automatic measurement of yarn hairiness based on the improved mrmrf segmentation algorithm. Journal of the Textile Institute, 109(6), 740-749.
[4] Rathee, G., Sharma, A., Saini, H., Kumar, R., & Iqbal, R. (2019). A hybrid framework for multimedia data processing in IoT-healthcare using blockchain technology. Multimedia Tools and Applications, 1-23.
[5] Sharma, A., Tomar, R., Chilamkurti, N., & Kim, B. G. (2020). Blockchain based smart contracts for internet of medical things in e-healthcare. Electronics, 9(10), 1609.
[6] Baqersad, J., Poozesh, P., Niezrecki, C., & Avitabile, P. (2017). Photogrammetry and optical methods in structural dynamics–A review. Mechanical Systems and Signal Processing, 86, 17-34.
[7] Rathee, G., Sharma, A., Saini, H., Kumar, R., & Iqbal, R. (2019). A hybrid framework for multimedia data processing in IoT-healthcare using blockchain technology. Multimedia Tools and Applications, 1-23.
[8] Son, K. S., Jeon, H. S., Park, J. H., & Park, J. W. (2015). Vibration displacement measurement technology for cylindrical structures using camera images. Nuclear Engineering and Technology, 47(4), 488-499.
[9] Endo, M. T., Montagnoli, A. N., & Nicoletti, R. (2015). Measurement of shaft orbits with photographic images and sub-sampling technique. Experimental Mechanics, 55(2), 471-481.
[10] Kaushik, M., Gupta, S. H., & Balyan, V. (2019, March). Evaluating Threshold Distance by Using Eigen Values and Analyzing Its Impact on the Performance of WBAN. In 2019 6th International Conference on Signal Processing and Integrated Networks (SPIN) (pp. 864-867). IEEE.
[11] Dhiman, G., Oliva, D., Kaur, A., Singh, K. K., Vimal, S., Sharma, A., & Cengiz, K. BEPO: A novel binary emperor penguin optimizer for automatic feature selection. Knowledge-Based Systems, 211, 106560.
[12] Xu, F. (2019). Accurate measurement of structural vibration based on digital image processing technology. Concurrency & Computation Practice & Experience, 31(10), e4767.1-e4767.10.
[13] Gao, M., Wang, X., Zhu, S., & Guan, P. (2020). Detection and segmentation of cement concrete pavement pothole based on image processing technology. Mathematical Problems in Engineering, 2020(6), 1-13.
[14] Gao, X., Song, X., Zheng, Z., Xie, M., & Huang, S. (2020). Misalignment measurement of orbital angular momentum signal based on spectrum analysis and image processing. IEEE Transactions on Antennas and Propagation, 68(1), 521-526.
[15] Park, J. W., Lee, J. J., Jung, H. J., & Myung, H. (2010). Vision-based displacement measurement method for high-rise building structures using partitioning approach. Ndt & E International, 43(7), 642-647.
[16] Ye, X. W., Dong, C. Z., & Liu, T. (2016). Image-based structural dynamic displacement measurement using different multi-object tracking algorithms. Smart Structures and Systems, 17(6), 935-956.
[17] Becker, T. H., Mostafavi, M., Tait, R. B., & Marrow, T. J. (2012). An approach to calculate the J-integral by digital image correlation displacement field measurement. Fatigue & Fracture of Engineering Materials & Structures, 35(10), 971-984.
[18] Ye, X. W., Yi, T. H., Dong, C. Z., Liu, T., & Bai, H. (2015). Multi-point displacement monitoring of bridges using a vision-based approach. Wind and Structures, 20(2), 315-326.
[19] Quan, C., Tay, C. J., Sun, W., & He, X. (2008). Determination of three-dimensional displacement using two-dimensional digital image correlation. Applied optics, 47(4), 583-593.
[20] Kim, S. W., Jeon, B. G., Kim, N. S., & Park, J. C. (2013). Vision-based monitoring system for evaluating cable tensile forces on a cable-stayed bridge. Structural Health Monitoring, 12(5-6), 440-456.
[21] Fukuda, Y., Feng, M. Q., Narita, Y., Kaneko, S. I., & Tanaka, T. (2013). Vision-based displacement sensor for monitoring dynamic response using robust object search algorithm. IEEE Sensors Journal, 13(12), 4725-4732.
[22] You, D., Gao, X., & Katayama, S. (2014). Monitoring of high-power laser welding using high-speed photographing and image processing. Mechanical Systems and Signal Processing, 49(1-2), 39-52.
[23] Chen, J. G., Wadhwa, N., Cha, Y. J., Durand, F., Freeman, W. T., & Buyukozturk, O. (2015). Modal identification of simple structures with high-speed video using motion magnification. Journal of Sound and Vibration, 345, 58-71.
[24] Cha, Y.J.; Chen, J.G. (2015). Buyukozturk, O. Motion magnification based damage detection using high speed video. In Proceedings of the 10th International Workshop on Structural Health Monitoring (IWSHM), Palo Alto, CA, USA, 1–3 September 2015.
[25] Dehghani, M., Montazeri, Z., Dhiman, G., Malik, O. P., Morales-Menendez, R., Ramirez-Mendoza, R. A., ... & Parra-Arroyo, L. (2020). A spring search algorithm applied to engineering optimization problems. Applied Sciences, 10(18), 6173.
[26] Kaushik, M., Gupta, S. H., & Balyan, V. (2020). Power optimization of invivo sensor node operating at terahertz band using PSO. Optik, 202, 163530.
[27] Gautama, T., & Van Hulle, M. A. (2002). A phase-based approach to the estimation of the optical flow field using spatial filtering. IEEE Transactions on Neural Networks, 13(5), 1127-1136.
[28] Lei, X., Jin, Y., & Guo, J. (2015). Vibration extraction based on fast NCC algorithm and high-speed camera. Applied optics, 54(27), 8198-8206.
[29] Evangelidis, G. D., & Psarakis, E. Z. (2008). Parametric image alignment using enhanced correlation coefficient maximization. IEEE Transactions on Pattern Analysis and Machine Intelligence, 30(10), 1858-1865.
[30] Dhiman, G. (2019). ESA: a hybrid bio-inspired metaheuristic optimization approach for engineering problems. Engineering with Computers, 1-31.

[31] Dehghani, M., Montazeri, Z., Givi, H., Guerrero, J. M., & Dhiman, G. (2020). Darts game optimizer: A new optimization technique based on darts game. Int. J. Intell. Eng. Syst, 13, 286-294.
[32] Wei, X., Jiang, S., Li, Y., Li, C., Jia, L., & Li, Y. (2019). Defect detection of pantograph slide based on deep learning and image processing technology. IEEE Transactions on Intelligent Transportation Systems, 1-12.
[33] Usman, M., Zabit, U., Bernal, O. D., Raja, G., & Bosch, T. (2019). Detection of multimodal fringes for self-mixing-based vibration measurement. IEEE Transactions on Instrumentation and Measurement, 258-267.
[34] Tian, W., Li, Y., Hu, C., Li, Y., & Zeng, T. (2019). Vibration measurement method for artificial structure based on mimo imaging radar. IEEE Transactions on Aerospace and Electronic Systems, 56(1), 748-760.
[35] Aghaamiri, R., Hajnayeb, A., & Shirazi, K. H. (2020). Metrology and measurement systems vibration measurement for crack and rub detection in rotors. Metrology and Measurement Systems, 27(1), 65-80.
[36] Dickinson, A. S., Taylor, A. C., Ozturk, H., & Browne, M. (2011). Experimental validation of a finite element model of the proximal femur using digital image correlation and a composite bone model. Journal of biomechanical engineering, 133(1).
[37] Mathieu, F., Hild, F., & Roux, S. (2012). Identification of a crack propagation law by digital image correlation. International Journal of Fatigue, 36(1), 146-154.